Journal of Sedimentary Research

Journal of Sedimentary Research, 2013, v. 83, 522–530
Research Article
DOI: 10.2110/jsr.2013.29

QUARTZ CEMENTATION HISTORY OF SANDSTONES REVEALED BY HIGH-RESOLUTION SIMS OXYGEN ISOTOPE ANALYSIS

JOSEPH HARWOOD,[1] ANDREW C. APLIN,*[1] CLAIRE I. FIALIPS,†[1] JAMES E. ILIFFE,[2] REINHARD KOZDON,[3] TAKAYUKI USHIKUBO,[3] AND JOHN W. VALLEY[3]

[1]*School of Civil Engineering and Geosciences, Newcastle University, Newcastle upon Tyne, NE1 7RU, U.K.*
[2]*BP Exploration and Production, Sunbury-on-Thames, U.K.*
[3]*WiscSIMS, Department of Geoscience, University of Wisconsin, Madison, Wisconsin 53706, U.S.A.*
e-mail: a.c.aplin@durham.ac.uk

ABSTRACT: **Evaluating the timing and origin of quartz cement is central to understanding how porosity is lost in sandstones during burial. Kinetic models of quartz cementation have been calibrated using large–scale datasets but have never been tested at the microscopic level at which cement forms. Here, we use high-precision, *in situ* oxygen isotope analyses on sandstone from the Jurassic Ness Formation from the North Sea to reveal the growth history of single quartz overgrowths to a resolution of 2 μm. Measured $\delta^{18}O_{(cement)}$ range from +28 to +20‰ V-SMOW in early to late cement and are consistent with quartz cementation models that propose the bulk of quartz precipitates as a continuous process beginning at 60–70 °C. Quantitative X-ray Diffraction analyses and clay mineralogical analysis of interbedded shales are inconsistent with a silica source from shale, implying that silica for the cement is sourced internally to the sand. These isotope data are broadly consistent with predictive, conceptual quartz cementation models and provide a critical link from micron-scale measurements to basin-scale predictions and observations.**

INTRODUCTION

Since quartz is the most abundant diagenetic mineral in sandstones, constraining the rates and mechanisms of quartz cementation is fundamental to quantifying changes in the physical properties of sandstones during burial, and central to the prediction of the quality of many petroleum reservoirs (Worden and Morad 2000). Many studies have thus attempted to evaluate the temperature and timing of precipitation as well as the origin of silica during the "cementation window," typically through the combined use of fluid-inclusion (Haszeldine et al. 1984; Walderhaug 1994; Wilkinson et al. 1998), petrographic (Blanche and Whitaker 1978; Hogg et al. 1992; Oelkers et al. 1996), and isotopic investigations (Brint et al. 1991; Aplin and Warren 1994; Williams et al. 1997; Girard et al. 2001; Marchand et al. 2002).

By combining data on fluid inclusions and cement abundance acquired from sandstones buried with well-defined thermal histories to a range of temperatures, Walderhaug (1994) estimated the rate of quartz cementation as a function of time, temperature, and quartz surface area. These data form the basis of commonly used kinetic models of quartz cementation (Walderhaug 1996; Lander and Walderhaug 1999; Lander et al. 2008). Furthermore, since (a) quartz cement is infrequently observed in sandstones which have never been buried to greater than 70–80°C and (b) fluid inclusions in quartz overgrowths seldom reveal homogenization temperatures below 70–80°C, conceptual models commonly assume that quartz cementation has an effective threshold temperature of around 70–80°C (Lander and Walderhaug 1999; Walderhaug 2000). Some authors (Girard et al. 2001; Marchand et al. 2002) propose an episodic cementation process once cementation has been initiated, whilst others (Walderhaug 1996; Oelkers et al. 2000) suggest that cementation is a continuous process, with cement developing as a function of both temperature and quartz surface area, and with most cement precipitating between 100 and 120°C.

Although many studies suggest that silica is sourced internally within the sandstone as a result of quartz stylolitization, other potential silica sources have also been recognized (see reviews by McBride 1989 and Worden and Morad 2000). Internally, other possible silica sources include recrystallization of biogenic silica (Jahren and Ramm 2000; Goldstein and Rossi 2002; Haddad et al. 2006) and feldspar dissolution (Bjørlykke and Egeberg 1993). Other authors propose a more open chemical system in which silica may be transported from local shale units (e.g., Day-Stirrat et al. 2010); in this scenario, clay-mineral reactions, most notably the transformation of smectite to illite (Hower et al. 1976; van de Kamp 2008), are thought to contribute towards the silica budget.

To date, it has proved difficult to validate the precipitation kinetics established for these broadly based quartz cementation models on the microscopic scale at which cement forms. In principle, detailed profiles of either fluid-inclusion and oxygen isotopic data, or both, across single overgrowths can be used to constrain cementation history. However, fluid inclusions occur mainly close to the boundary of overgrowths and detrital grains, and thus constrain only the early phase of cementation (Osborne and Haszeldine 1993). Early isotopic studies isolated whole overgrowths and could not generate temporal data (Lee and Savin 1985; Brint et al. 1991; Aplin and Warren 1994), whilst neither the resolution (20–30 μm)

* Present Address: Department of Earth Sciences, Durham University, Durham, DH1 3LE, U.K.
† Present Address: TOTAL SA, CSTJF, Avenue Larribau, 64018 Pau, France

Published Online: June 2013
 1527-1404/13/083-522/$03.00

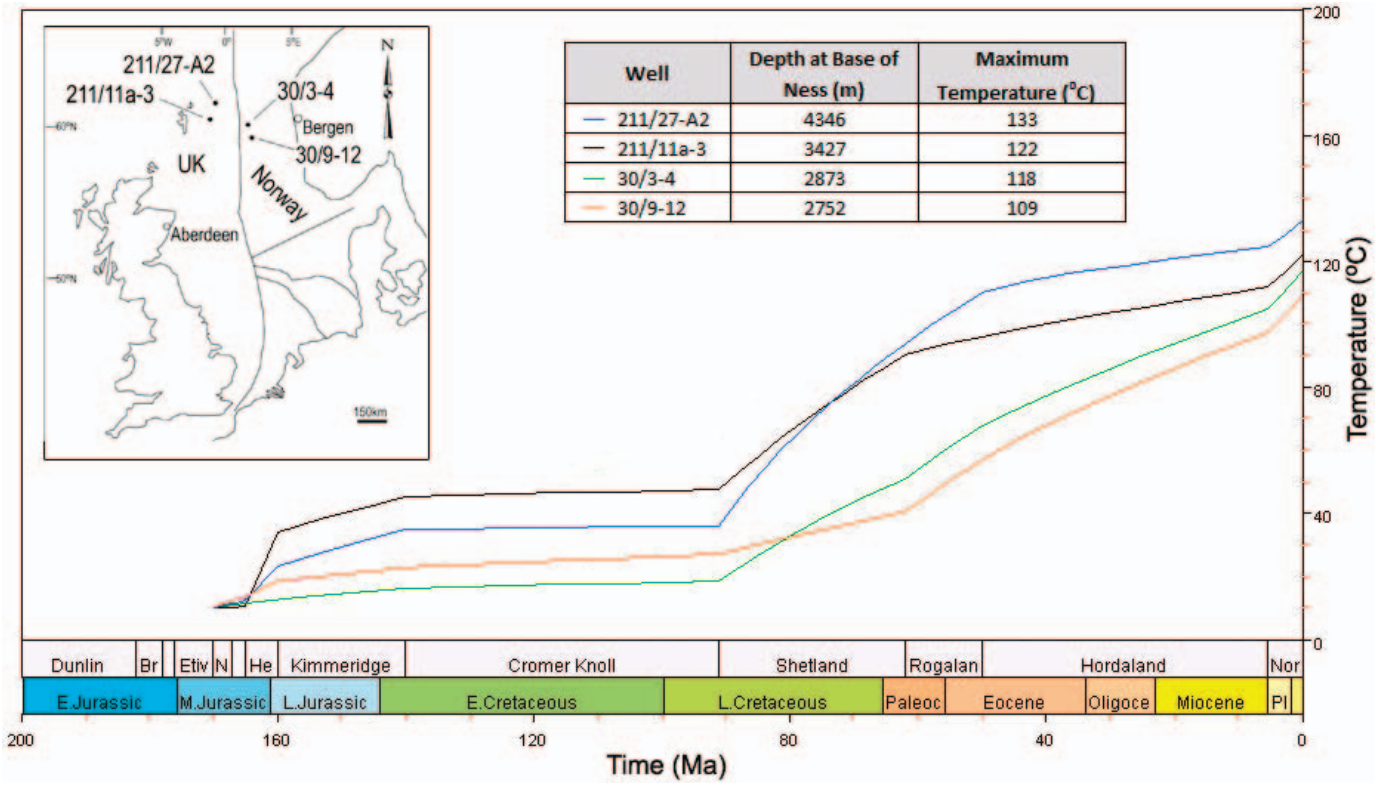

FIG. 1.—Thermal history of the Ness Formation constructed using Genesis 4.8 and calibrated with vitrinite reflectance and measured temperature data. Depths are in meters below Kelly-Bushing.

nor the precision (± 2‰; 2SD) of earlier *in situ* studies by single-collector secondary ion mass spectrometer (SIMS) were sufficient to constrain growth histories (Graham et al. 1996; Williams et al. 1997; Lyon et al. 2000; Girard et al. 2001; Marchand et al. 2002).

In this study, we present high-precision, high-accuracy, high-spatial-resolution SIMS analyses on quartz overgrowths from a Jurassic sandstone from the North Sea; similar sandstones have been extensively characterized in previous studies with analysis of bulk samples (Hogg et al. 1992; Hogg et al. 1995; Wilkinson et al. 1998; Walderhaug 2000; Marchand et al. 2002). This study reports the first use of a 2 μm analysis spot across individual quartz overgrowths, a method that delineates small-scale oxygen isotope zonation and provides a previously unattainable record of quartz precipitation history. The isotopic data are combined with petrographic data from the sands and mineralogical data from local shale units to (a) evaluate quartz cementation histories, (b) provide data which help to test commonly used quartz cementation models, and (c) constrain likely sources of silica and thus the openness of the sand-shale diagenetic system.

MATERIALS AND METHODS

Samples of interbedded sandstone and shale were selected from four wells penetrating the Ness Formation, part of the Middle Jurassic Brent Group in the East Shetland Basin and the northern Viking Graben of the northern North Sea (Fig. 1). The Brent Group was deposited in a range of shallow marine and deltaic environments and comprises five units: the Broom, Rannoch, Etive, Ness, and Tarbert formations (e.g., Brown and Richards 1989; Richards 1992). The post-Brent sediment succession is fully marine. The object of this study, the Ness Formation, includes interbedded sandstone, siltstone, and shale, and was deposited in a range of delta-plain and coastal-plain environments (e.g., Brown and Richards 1989; Livera 1989; Richards 1992). Composite logs from the wells sampled in this study suggest that the sand-to-shale ratio in the Ness Formation is typically 50:50, although a small number of thin coal beds are present. In hand specimen, sand is fine to medium grained and commonly contains varying amounts of silt- and clay-grade matrix material.

The quantitative mineralogy of 14 shale units from the four wells was determined using X-ray diffraction. All samples were prepared using the spray-drying technique described by Hillier (2003) with a 20% corundum standard added to each sample. All analyses were carried out on randomly oriented powders using Cu-Kα radiation on a PANalytical X'Pert Pro MPD diffractometer, fitted with an X'Celerator and a secondary monochromator. All analyses were run over a range of 2–70° 2θ with a nominal step size of 0.0167° 2θ and time per step of 100 seconds. The quantitative analysis of the different mineral constituents was completed using FullPat, a full-pattern mineral quantification package developed by Chipera and Bish (2002).

The < 2 μm fractions of the crushed shale samples were separated by centrifugation of dilute suspensions, prepared as oriented mounts and analyzed from 2 to 40° 2θ after successive (1) air drying, (2) ethylene glycol saturation (at 60°C for 24 hours), and (3) heat treatment to 375°C (for 1–2 hours). The percentage of illite within the illite–smectite mixed-layer phases (I/S) were determined using the methodology of Moore and Reynolds (1997).

For the eight sandstones, total volumes of quartz, porosity, non-quartz minerals, and quartz cement were quantified using a combination of back-scattered electron (BSE) and cathodoluminescence (SEM-CL) microscopy using a Philips/FEI XL30 Environmental Scanning Electron Microscope–Field Emission Gun (XL30 ESEM-FEG). Image analysis

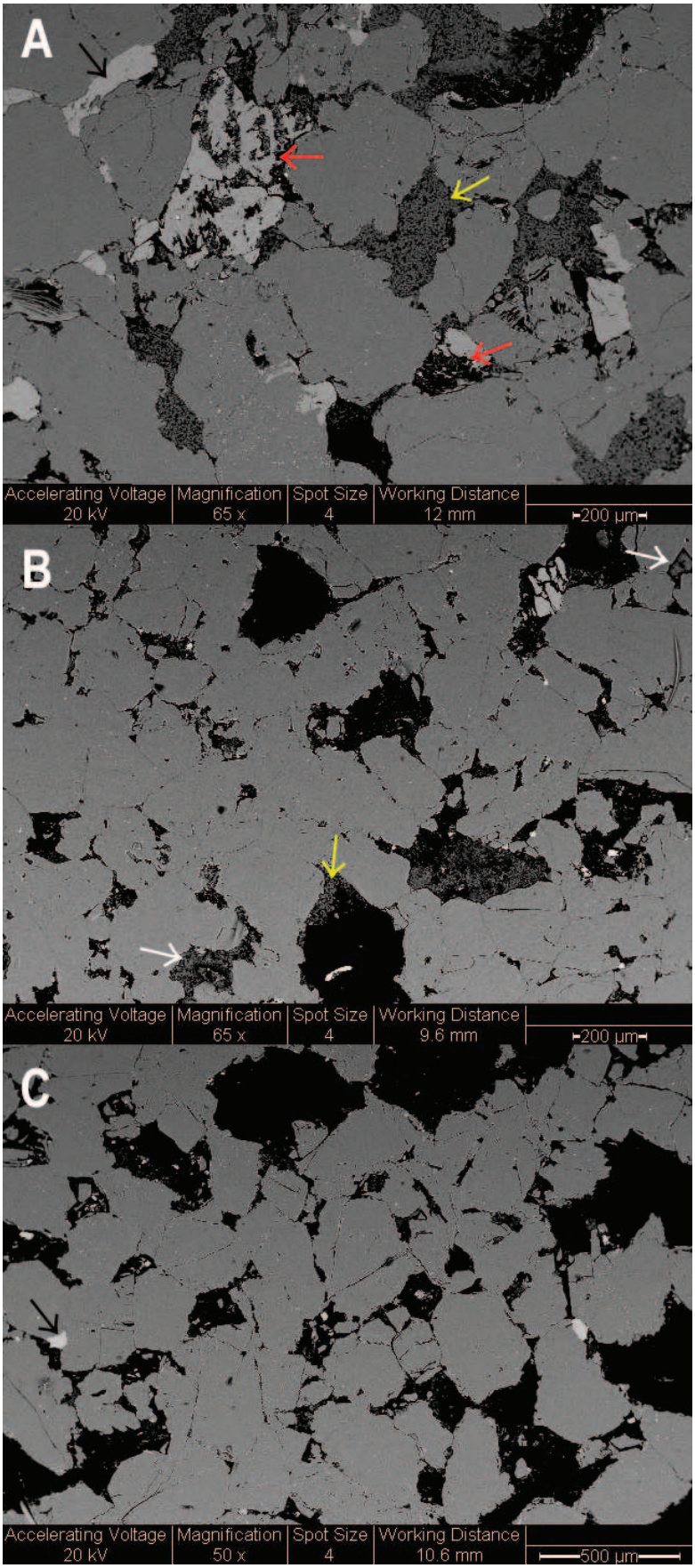

FIG. 2.—BSE images of Ness sandstones. **A)** Sample is taken from well 211/11a-3, **B**, **C)** Samples are taken from well 211/27-A2. Feldspar dissolution (red arrow), abundant kaolin (yellow arrow) as well as minor illite (white arrow) and calcite (black arrow) are evident. All mineral compositions are confirmed by SEM EDS.

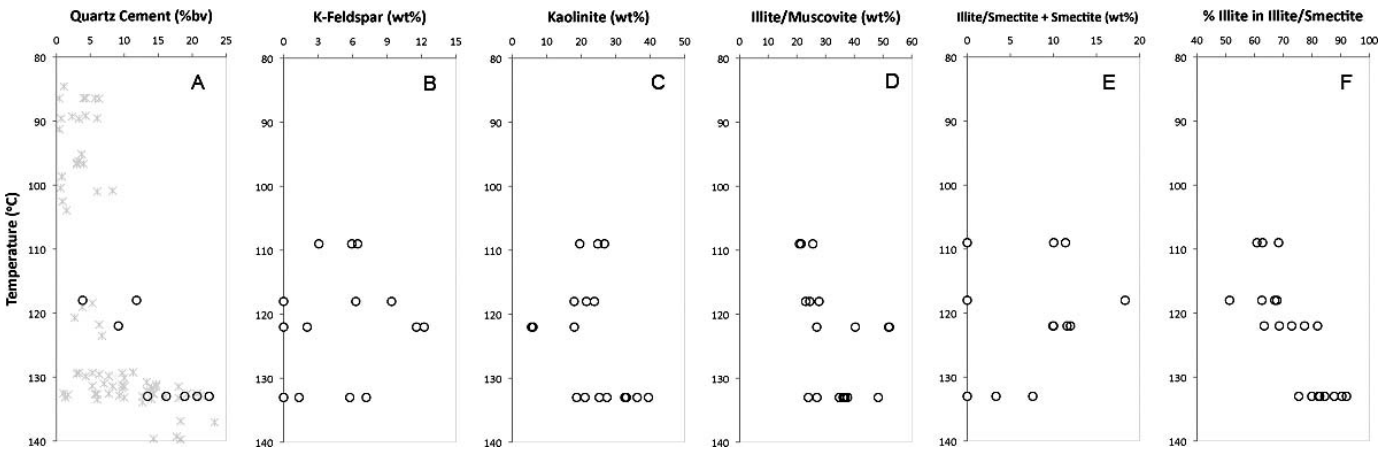

FIG. 3.—Mineralogical analysis of the Ness Formation. **A)** Percentage of quartz cement in Ness Formation sandstone based on image analysis of SEM-CL images. Gray crosses are data from similar North Sea Brent Group sandstones (Harris 1992; Walderhaug 1994). **B–E)** Quantitative bulk mineralogy of Ness shales. **F)** Percentage of illite in mixed layer illite–smectite of < 2 μm fraction of Ness shales.

was carried out according to methods described by Evans et al. (1994) and Cooper et al. (2000). The average grain size was determined by measuring the long axis of 100 randomly selected, non-ductile detrital grains.

Three samples were selected for secondary-ion mass spectrometer (SIMS) analysis, one from well 211/11a-3 and two from well 211/27-A2 (Fig. 2). Oxygen isotope ratios were measured on eleven separate overgrowths using a CAMECA IMS-1280 ion microprobe at the WiscSIMS Laboratory, University of Wisconsin–Madison (Kita et al. 2009). SEM-CL examination of the analysis pits enabled us to determine whether the analyzed volume comprised detrital or authigenic quartz, or a mixture of both. Analyses of detrital and mixed authigenic–detrital quartz are identified in the Supplementary Material (see Acknowledgments). Full analytical details can be found in Kelly et al. (2007), Page et al. (2007), Valley and Kita (2009), Kita et al. (2009), and Pollington et al. (2011).

Stratigraphic data were used in Genesis 4.8, a 1D thermal modeling software, to construct time–temperature histories for all wells. These histories were calibrated to present-day sample temperatures of 109, 118, 122, and 133°C (Fig. 1).

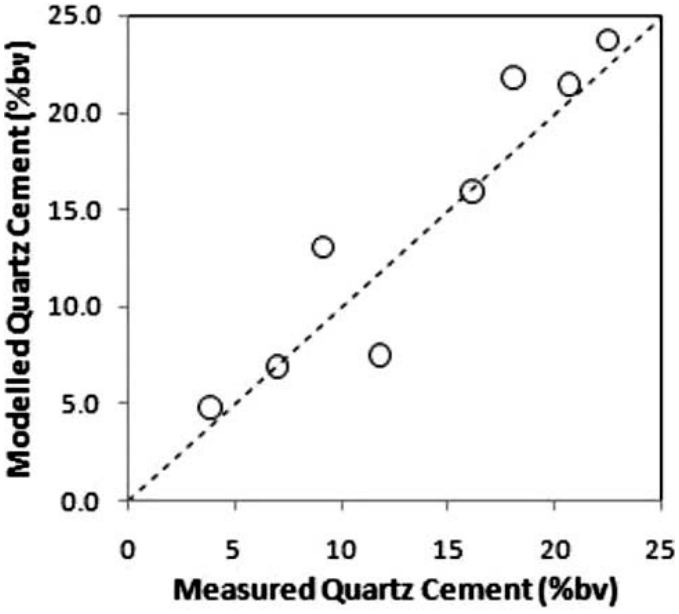

FIG. 4.—Measured quartz cement versus quartz cement predicted from Walderhaug's (1996) model.

Potential quartz cementation histories were constructed using Walderhaug's (1996) empirical kinetic model. This predicts the volume of quartz cement precipitated per unit time over a volume of, for example, 1 cm^3, as a function of temperature, quartz surface area, and porosity prior to the onset of cementation. Assumptions implicit in the model are that cementation starts at a threshold temperature and then occurs continuously through to maximum burial. In this work, we estimated quartz surface area through the quantitative petrographic analysis of per cent detrital quartz and quartz grain size. Initial porosity was taken to be the minus-cement porosity, and the time–temperature history was derived from the Genesis models. This allows the volume of cement to be calculated as a function of either time or temperature in a specified volume of sandstone. However, in order to compare the micron-scale $\delta^{18}O$ data with modeled cementation histories, we need to consider how individual overgrowths have developed through time. We have done this by assuming that (a) the relative rate of cementation at the scale of a single overgrowth is the same as the bulk rate predicted by Walderhaug's (1996) model over a given temperature interval, (b) growth occurs radially outwards from the detrital grain, and (c) growth starts around 80°C and continues to maximum (present-day) temperature.

RESULTS

Shale Composition

The main mineralogical components in the shales (Fig. 3) suggest that any potential mineralogical trends with temperature are concealed by sample heterogeneity. Phyllosilicates are dominated by illite/muscovite and kaolin, with lesser abundances of illite–smectite (I-S). Mixed layer I-S contains 64% I at 109°C, increasing to 82% at 133°C (Fig. 3F). K-feldspar is present at all temperatures, but in amounts varying between 0 and 12% (Fig. 3B).

Sandstone Composition

By bulk volume, the sandstone samples consist of 78–84% total quartz with a mean grain size of 250–300 μm; modal porosities range from 5 to 15% (bv). The non-quartz constituent largely comprises K-feldspar with minor calcite; illite and kaolin cements are also observed filling primary macroporosity. The replacement of feldspar by kaolin is seen commonly in all samples (Fig. 2). Quartz cement varies from 16 to 23% bv (Fig. 3A),

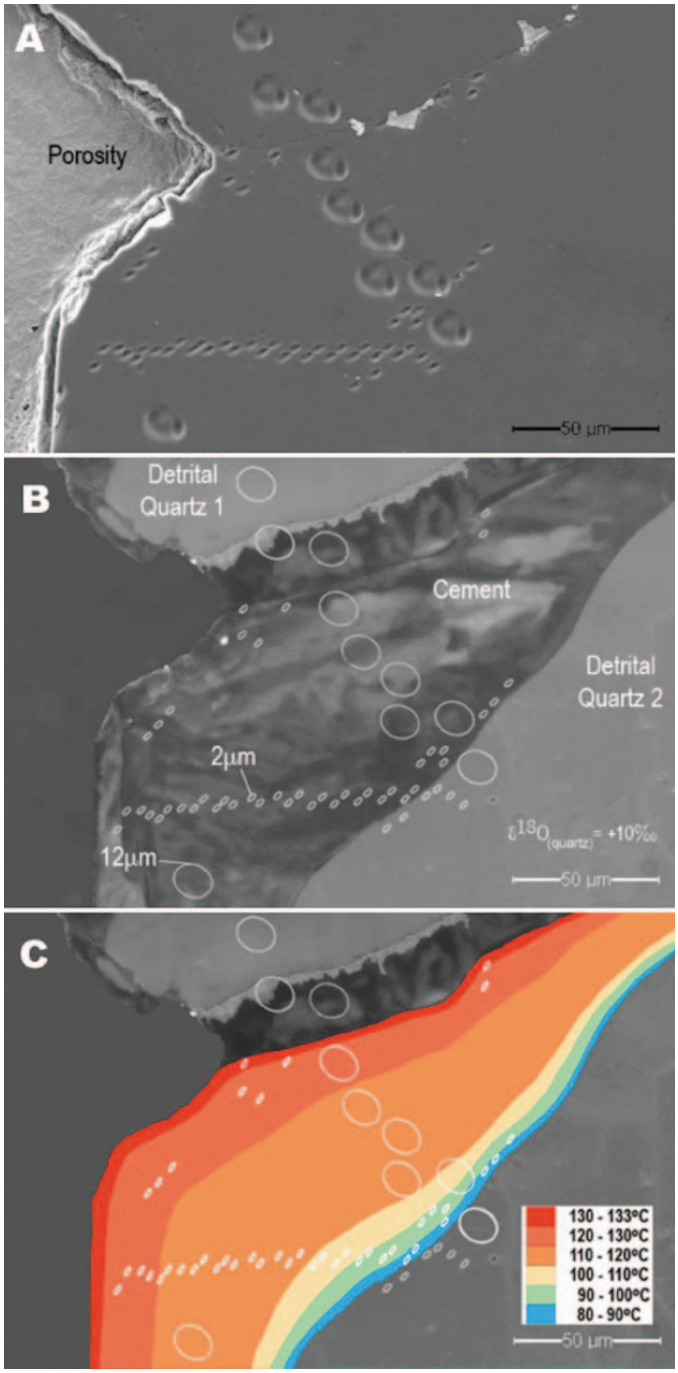

FIG. 5.—**A)** SE image showing 2 and 12 µm diameter ion microprobe pits generated from SIMS analysis of oxygen isotopes. **B)** SEM-CL image showing boundaries between detrital and authigenic quartz, a lighter luminescing rind on the detrital surface of the grain 1, and a darker rind on grain 2. **C)** Modeled cementation history based on kinetics described by Walderhaug (1996), assuming linear growth from the grain boundaries. Comparison with Part B shows the resolution to which cementation histories can be revealed with different SIMS spot sizes.

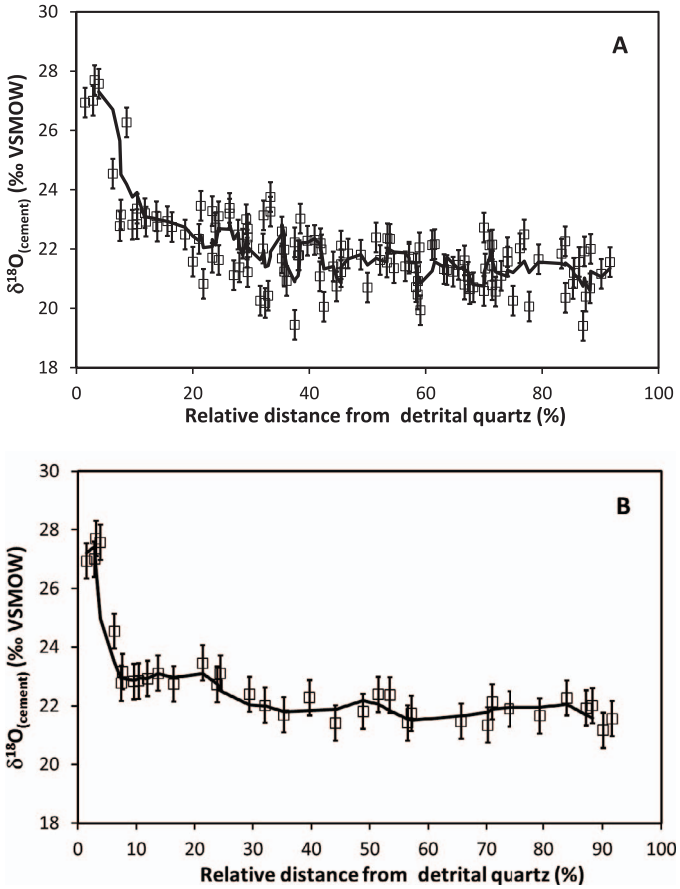

FIG. 6.—$\delta^{18}O_{(Cement)}$ vs. relative distance between detrital grain boundary and outer edge of overgrowth. **A)** All data from eleven overgrowths and a four-point moving average. **B)** 2 µm data from the single overgrowth shown in Figure 5, with a three-point moving average.

with more cement at higher temperatures. Measured volumes of quartz cement in the eight sandstone samples studied show reasonable agreement with the volumes predicted by Walderhaug's (1996) kinetic model (Fig. 4). SEM-CL shows very limited zonation in quartz overgrowths, although a thin zone of brighter luminescing, authigenic quartz is evident at the edge of detrital grain 1 and a darker 8 µm zone in grain 2 (Fig. 5B). SEM analysis also highlighted the widespread, incipient illitization of kaolin booklets. Furthermore, both fibrous illite and kaolin booklets are enclosed by authigenic quartz overgrowths throughout both samples, indicating that quartz continued to precipitate after the formation of illite and kaolin, and thus after the main phase of K-feldspar dissolution. Nodular calcite locally occludes porosity and predates quartz overgrowths. Similar paragenetic sequences were observed by both Glasmann et al. (1989) and Harris (1992) in other Brent sandstones.

Isotopic Composition of Quartz Cement

SIMS analyses were carried out over two sessions. Initially, 234 analyses were made with a 12-µm-diameter beam, of which 73 were made in the sample from well 211/11a-3 (122°C) and a further 161 were performed in the samples from well 211/27-A2 (Fig. 6); in total, 125 analyses were made on authigenic quartz. Sixty-eight bracketing analyses of the UWQ-1 quartz standard, mounted in the center of each thin section (Kelly et al. 2007), were used to calibrate analyses of $\delta^{18}O$ relative to V-SMOW and indicate a spot-to-spot precision of ± 0.4‰ (2SD). In a second session, 73 analyses were made using a 2 µm beam from a 200 µm × 200 µm area (Fig. 5A); the analytical precision with smaller spots was ± 0.7‰ (2SD). The sample size for each *in situ* 12 µm spot analysis is one million times smaller (ca. 2 ng vs. 2 mg) than in earlier studies of oxygen

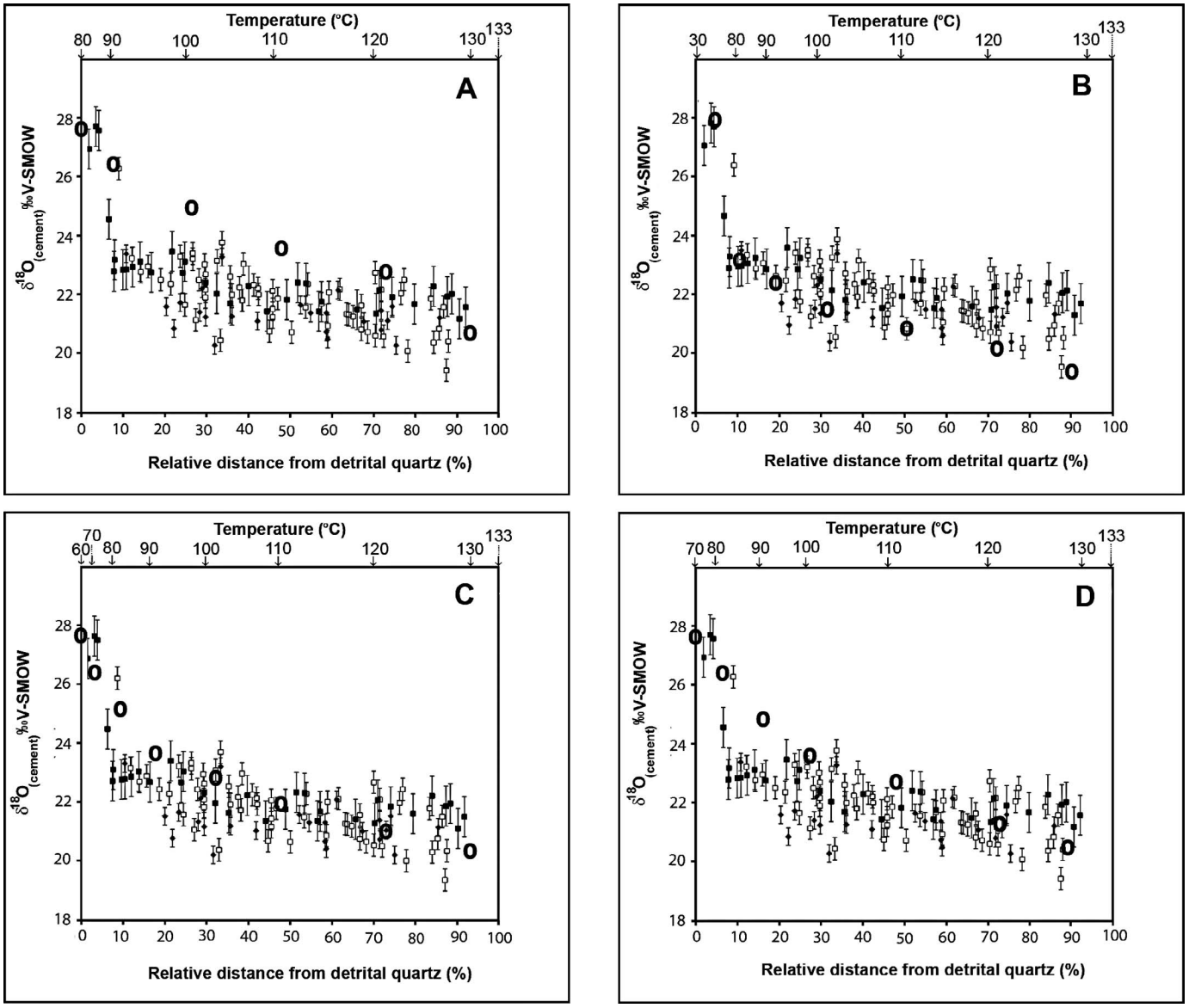

FIG. 7.—$\delta^{18}O_{(Cement)}$ vs. relative distance between detrital grain boundary and outer edge of overgrowth. Filled squares are 2 μm data and open squares are 12 μm data. The temperature vs. distance is calculated using quartz precipitation kinetics suggested by Walderhaug (1994). Whereas the analytical data in each of the four figures are identical, each figure has circles which show how the oxygen isotopic composition of quartz would change as a function of temperature and the isotopic composition of water. **A)** cementation occurs from 80 to 133°C in a water with a constant isotopic composition of 3.6‰; **B)** a thin zone of cement forms at 30°C in a water with $\delta^{18}O = -6.1‰$, and then between 80 and 133°C in a water which evolves from $\delta^{18}O = -1‰$ to 2.9‰; **C)** cementation occurs between 60 and 133°C in a water which evolves from $\delta^{18}O = 0.2‰$ to 2.9‰; **D)** cementation occurs between 70 and 133°C in a water which evolves from $\delta^{18}O = 2‰$ to 2.9‰. See text for further details.

isotope ratios that employed fluorination and gas-source mass spectrometry (Page et al. 2007). Nevertheless, the slow kinetics of quartz cementation at low temperatures means that even smaller beam sizes are required to resolve the few microns of cement that are predicted to precipitate in the early phases of cementation. For example, given a cementation history based on the kinetics described by Walderhaug (1996), cement has been built up in 10°C increments (Fig. 5C). It is apparent that even a 12 μm SIMS analysis spot cannot resolve cements formed around or below 80°C under these conditions. In this study, we therefore used a 2 μm isotopic analysis spot to generate a more detailed cementation history. All analyses of sample and standard are reported in order of analysis in the Supplementary Material.

Twenty-two analyses were taken from detrital grains across the two samples; $\delta^{18}O_{(Quartz)}$ averaged +10.6‰ V-SMOW, a value very different from that of the authigenic quartz but characteristic of detrital igneous quartz. In the absence of CL sector zoning, the initial assumption is that cementation has occurred in an essentially concentric fashion outwards from the edges of detrital quartz grains (e.g., Pollington et al. 2011). Oxygen isotope data are thus plotted as a function of the relative distance across the overgrowth (Figs. 6, 7). The data display a remarkable 8.4‰ range, between +19.3‰ and +27.7‰ V-SMOW, although the vast majority of the data are between +20 and +23.5‰. Five 2 μm spots taken within and close to the darker luminescing cement next to detrital grain 2 (Fig. 5B) have $\delta^{18}O_{(Cement)}$ values of +24.5 to +27.7‰, values which are also hinted at by the 12 μm data. Whereas it is clear that the two points at +27.0 and 27.7‰ are taken within the darker-luminescing zone, it is impossible to be certain if the two data points between +24.5 and +25.2‰ represent a mixed analysis of two isotopically distinct

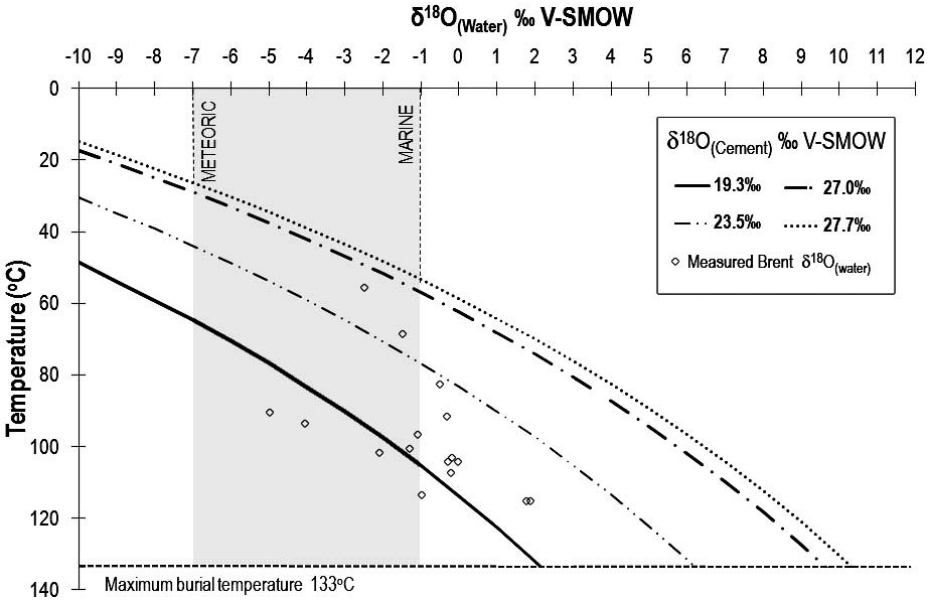

FIG. 8.—Plot of $\delta^{18}O_{(Water)}$ in equilibrium with quartz cement ($\delta^{18}O_{(Cement)}$ = 19.3‰, 23.5‰, 27.0‰, and 27.7‰, V-SMOW contours) as a function of temperature (Clayton et al. 1972). Jurassic meteoric (−7‰) and marine (−1‰) water compositions are indicated by the light shaded region. Modern Brent $\delta^{18}O_{(Water)}$ are represented by the diamonds (Warren and Smalley 1994).

zones—implying two phases of cementation—or represent part of a single, continuous cementation history which nevertheless generated two CL zones.

Beyond the isotopically heavy cement close to the detrital grain, the remaining data fall between +20 and +23.5‰ (Fig. 6A). Whilst there is variability in the data, perhaps reflecting the fact that the analyses were made on eleven overgrowths from two samples, a four-point moving average through the data suggests that the main trend is towards isotopically lighter later cement (Fig. 6A); there is no evidence for either cyclicity or major breaks in the data.

Given their typical thickness of 50–70 μm, only the 2 μm data can reveal detailed isotopic histories across individual overgrowths. Results for the 2 μm profile taken across the overgrowth in Figure 5 are reported in Figure 6B. The trends are similar to but smoother than those observed in the full dataset: a sharp decrease from +27.5 to +23.5‰ over the inner 10% of the overgrowth, with a further general decrease to around +21.3‰ close to the edge of the overgrowth. A three-point moving average through the data indicate some minor fluctuations in the data but reveal no evidence of either cyclicity or abrupt shifts.

DISCUSSION

Since $\delta^{18}O_{(Cement)}$ is a dual function of precipitation temperature and $\delta^{18}O_{(Water)}$ (Clayton et al. 1972), isotopic data alone cannot define unique cementation histories. However, they can be used in combination with $\delta^{18}O_{(Water)}$ values of −6 to −7‰ for Jurassic meteoric water, −1‰ for Jurassic seawater, and a range of +1.1 to +2.7‰ for present-day formation waters in other Brent sandstones (Egeberg and Aagaard 1989; Aplin and Warren 1994; Warren and Smalley 1994) to place some important constraints on cementation. Precipitation of the last-formed cement with $\delta^{18}O$ around +21‰ close to present-day burial temperature would occur in a formation water with $\delta^{18}O$ = +2.9‰, close to those seen in other Brent sands (Fig. 8). However, with a $\delta^{18}O_{(Cement)}$ of +27.7‰, if cementation started at 80°C (Walderhaug 1996), it would have to occur in a formation water with $\delta^{18}O$ = +3.6‰, markedly heavier than any Brent formation water measured to date. Continuing precipitation of quartz from 80 to 133°C in formation water with $\delta^{18}O$ = +3.6‰ would then result in $\delta^{18}O_{(Cement)}$ around 2‰ more positive than actually observed over much of the cementation history (Fig. 7A). To realistically model the observed quartz-cement isotope data, the oxygen isotopic composition of the formation waters would also need to reduce from +3.6‰ at 80°C to around +3.1‰ at 133°C. Since the oxygen isotope composition of formation waters generally evolve to *more* positive values with burial as a result of water–rock reactions (e.g., Aplin and Warren 1994), the assumed value of heavier waters (initial $\delta^{18}O$ = 3.6‰) during earlier diagenesis is unlikely.

It is more probable that quartz cementation began below the 70–80°C threshold recognized by current cementation models, as also suggested in several previous studies (Morad et al. 1994; Vagle et al. 1994; Kraishan et al. 2000; Marchand et al. 2002; Kelly et al. 2007; Pollington et al. 2011). Since $\delta^{18}O_{(Cement)}$ is a dual function of temperature and $\delta^{18}O_{(Water)}$, the isotopic data are inevitably consistent with several scenarios. The early, isotopically heavy cement could have formed in Jurassic meteoric waters (close to −6‰) at temperatures around 30°C, with the rest of the cement forming between 80 and 130°C in a water which as a result of water–rock interaction evolved isotopically from a value of −1.0‰ (close to seawater) to +2.9‰ (close to values currently observed in Brent sandstones in this region; Fig. 7B). In this case, silica for the early cement could have been sourced from the kaolinization of feldspars, a process observed both in our samples (Fig. 2) and by others in the Brent delta (e.g., Wilkinson et al. 2006). Indeed, Wilkinson et al. (2006) showed that $\delta^{18}O$ values for Brent vermiform kaolin are consistent with formation at temperatures below 40°C. On the other hand, the petrographic evidence for a distinctly luminescing early phase of cement resulting from the silica released from K-feldspar dissolution (e.g., Kraishan et al. 2000) is weak.

Another possible source for the high-$\delta^{18}O$ early cement is the recrystallization of biogenic silica (Jahren and Ramm 2000; Goldstein and Rossi 2002; Haddad et al. 2006), for example at 50°C from Jurassic seawater (−1‰) or at lower temperatures from mixed meteoric water and seawater (Fig. 8). Sands containing biogenic silica generally are deposited in marine environments, whereas the Ness is nonmarine. Nevertheless, coals and shales in the Ness testify to a humid, swampy environment in which opaline freshwater algae could have existed. However, although Mackenzie and Gees (1971) successfully precipitated small amounts of quartz at low temperatures from seawaters supersaturated with respect to quartz, this reaction results in the formation of microquartz (e.g., Weibel et al. 2010), for which there is no textural evidence in these samples.

We suggest that the isotopic data are most consistent with a conceptual model in which quartz cement formed continuously from temperatures of 60–70°C to the present maximum of 130°C. Since the isotopic data reflect both temperature and the isotopic ratio of the water from which quartz precipitated, we accept that more complex models might also fit the data. However, without either (a) strong petrographic evidence for a separate phase of early quartz cementation or (b) strong petrographic and isotopic evidence for discontinuous cementation at higher temperatures, such models will not be considered further. Assuming that cementation proceeded according to the kinetic model proposed by Walderhaug (1996), the isotopic composition of water would have evolved to match the observed isotopic data for the cement (Fig. 7). In one model, cementation starts at 60°C, and in the second, at 70°C. At 60°C, quartz with $\delta^{18}O$ = +27.8‰ would have precipitated from a water with $\delta^{18}O$ = +0.2‰, close to that of seawater and slightly lighter than the range currently observed for regional Brent formation waters (+1.1 to +2.7‰). The rest of the quartz isotopic data can be modeled quite well by precipitation from a water which evolves steadily from $\delta^{18}O$ = +0.2‰ at 60°C to + 2.9‰ at 133°C (Fig. 7C). The trend to isotopically more positive waters with burial is consistent with a relatively closed system in which clay minerals such as smectite are recrystallizing to illite, typically over a temperature range of 60–130°C (Aplin and Warren 1994).

In a second model, the isotopically heavy quartz cement precipitates from a water with $\delta^{18}O$ = +2.0‰ at 70°C, evolving slightly to +2.9‰ at 130°C (Fig. 7D). This model also fits much of the isotopic data for quartz, although it does not capture the very rapid isotopic change in the earliest phase of cementation. Overall, the petrographic data, combined with the isotopic trends within individual overgrowths and including the isotopically heavy cement, appear most consistent with a model in which quartz cement forms continuously from a threshold temperature of 60–70°C through to maximum burial (Ajdukiewicz and Lander 2010). In this study, quartz precipitated from waters which evolved as a result of water–rock interaction during burial (Aplin and Warren 1994), from a composition close to that of seawater to the more positive $\delta^{18}O$ values presently observed in the Brent (Fig. 8).

A number of possible silica sources may contribute to the cementation process (Worden and Morad 2000). The most plausible external source is the silica released from the illitization of smectite between 80°C and 140°C (Hower et al. 1976; Lynch et al. 1997; Peltonen et al. 2009). Here, observations from interbedded shales suggest that they cannot source the required silica. Wireline log data show that the shales constitute up to 50% of the total Ness Formation. Quantitative X-ray diffraction (QXRD) indicates that I-S constitutes a maximum of 18% of the shales, and that between 109 and 130°C, the temperature range over which there is substantial quartz cementation, the %S in I-S reduces from 35% to 15%. Using balanced equations similar to those published by Van de Kamp (2008), the maximum cement which could be generated from illitization is 2% bv, compared to the actual increase of typically 10% bv. Furthermore, this calculation presupposes complete export of the silica released from illitization; since others have documented authigenic quartz forming within shales through the zone of illitization (Peltonen et al. 2009; Thyberg et al. 2010), this situation is extremely unlikely.

Without a sufficient external source of silica, an internal source would require dissolution at stylolites and/or individual grain contacts containing illitic clay or mica. However, we see no evidence for pressure solution in the four examined thin sections, thus requiring silica transport on a scale larger than a few centimeters.

CONCLUSIONS

Over the past twenty years, petrographic, isotopic, and fluid inclusion data have been variously combined to propose either continuous or discontinuous quartz cementation histories in sandstones. Here, we have studied quartz cementation in Jurassic Ness Formation sandstones which are currently at maximum burial and have undergone a simple and continuous burial history. On a thin-section scale, the measured volumes of quartz cement are reasonably well predicted by Walderhaug's (1996) model which estimates the rate of quartz cementation as a function of time, temperature, and quartz surface area. Micron-scale oxygen isotope data on individual quartz overgrowths are consistent with the same model, supporting the idea that quartz cementation in these sandstones was a continuous process which can be predicted by quite simple kinetics. The combined petrographic and isotopic data can be interpreted as a process in which quartz cement formed continuously from 60–70°C to the current maximum temperature of 130°C in a highly restricted system within which waters evolved isotopically as a result of water–rock reactions, most probably clay-mineral recrystallization within interbedded shales. The bulk of silica must be sourced internally within the sands and cannot, based on mass-balance considerations, be sourced from reactions in interbedded shales. Most of the silica is interpreted to have been derived from dissolution at stylolites and individual grain contacts, a process which is interpreted to require transport at scales of a centimeter or greater. Since Walderhaug's (1996) original kinetic model was developed from broad observations of quartz cement volumes measured on many thin sections from a range of North Sea sandstones, our results help to form a process-based link from the scale of the individual overgrowth through to the thin section and then to the basin scale.

ACKNOWLEDGMENTS

The British Geological Survey is thanked for supplying all samples, and BP Exploration for providing data required for thermal modeling. Thin sections were made by Trevor Whitfield. Pauline Carrick (Newcastle University) and John Fournelle (University of Wisconsin–Madison) provided assistance with SEM imaging. This project was funded by an EPSRC-CASE Studentship in association with BP Exploration (CASE/CAN/06/54) and (BPX/PAT/RB/50686). WiscSIMS is partly supported by the National Science Foundation (EAR03-19230, 07-44079, 10-53466). Thoughtful reviews by Olav Walderhaug, Richard Worden, and an anonymous reviewer are much appreciated, as is the detailed editorial pen of John Southard. Supplemental Material is available from JSR′s Data Archive: http://sepm.org/pages.aspx?pageid=229.

REFERENCES

Ajdukiewicz, J.M., and Lander, R.H., 2010, Sandstone reservoir quality prediction: the state of the art: American Association of Petroleum Geologists, Bulletin, v. 94, p. 1083–1091.

Aplin, A.C., and Warren, E.A., 1994, Oxygen isotopic indications of the mechanisms of silica transport and quartz cementation in deeply buried sandstones: Geology, v. 22, p. 847–850.

Bjørkum, P.A., 1996, How important is pressure in causing dissolution of quartz in sandstones?: Journal of Sedimentary Research, v. 66, p. 147–154.

Bjørlykke, K., and Egeberg, P.K., 1993, Quartz cementation in sedimentary basins: American Association of Petroleum Geologists, Bulletin, v. 77, p. 1538–1548.

Blanche, J.B., and Whitaker, J.H.M., 1978, Diagenesis of part of the Brent Sand Formation (Middle Jurassic) of the northern North Sea Basin: Geological Society of London, Journal, v. 135, p. 73–82.

Brint, J.F., Hamilton, P.J., Haszeldine, R.S., Fallick, A.E., and Brown, S., 1991, Oxygen isotopic analysis of diagenetic quartz overgrowths from the Brent Sands: a comparison of two preparation methods: Journal of Sedimentary Petrology, v. 61, p. 527–533.

Brown, S., and Richards, P.C., 1989, Facies and development of the Middle Jurassic Brent Delta near the northern limit of its progradation, UK North Sea, *in* Whateley, M.K.G., and Pickering, K.T., eds., Deltas: Sites and Traps for Fossil Fuels: Geological Society of London, Special Publication 41, p. 253–267.

Chipera, S.J., and Bish, D.L., 2002, FULLPAT: a full-pattern quantitative analysis program for X-ray powder diffraction using measured and calculated patterns: Journal of Applied Crystallography, v. 35, p. 744–749.

Clayton, R.N., O'Neil, J.R., and Mayeda, T.K., 1972, Oxygen isotope exchange between quartz and water: Journal of Geophysical Research, v. 77, p. 3057–3067.

Cooper, M.R., Evans, J., Flint, S.S., Hogg, A.J.C., and Hunter, R.H., 2000, Quantification of detrital, authigenic and porosity components of the Fontainebleau Sandstone: A comparison of conventional optical and combined scanning electron microscope–based methods of modal analyses, *in* Worden, R.H., and Morad, S., eds., Quartz Cementation in Sandstones: International Association of Sedimentologists, Special Publication 29, p. 89–101.

Day-Stirrat, R.J., Milliken, K.L., Dutton, S.P., Loucks, R.G., Hillier, S., Aplin, A.C., and Schleicher, A.M., 2010, Open-system chemical behavior in deep Wilcox Group mudstones, Texas Gulf Coast, USA: Marine and Petroleum Geology, v. 27, p. 1804–1818.

Egeberg, P.K., and Aagaard, P., 1989, Origin and evolution of formation waters from oil fields on the Norwegian shelf: Applied Geochemistry, v. 4, p. 131–142.

Evans, J., Hogg, A.J.C., Hopkins, M.S., and Howarth, R.J., 1994, Quantification of quartz cements using combined SEM, CL, and image analysis: Journal of Sedimentary Research v. A 64, p. 334–338.

Girard, J.P., Munz, I.A., Johansen, H., Hill, S., and Canham, A., 2001, Conditions and timing of quartz cementation in Brent reservoirs, Hild Field, North Sea: constraints from fluid inclusions and SIMS oxygen isotope microanalysis: Chemical Geology, v. 176, p. 73–92.

Glasmann, J.R., Clark, R.A., Larter, S., Briedis, N.A., and Lundegard, P.D., 1989, Diagenesis and hydrocarbon accumulation, Brent Sandstone (Jurassic), Bergen High Area, North Sea: American Association of Petroleum Geologists, Bulletin, v. 73, p. 1341–1360.

Goldstein, R.H., and Rossi, C., 2002, Recrystallization in quartz overgrowths: Journal of Sedimentary Research, v. 72, p. 432–440.

Graham, C.M., Valley, J.W., and Winter, B.L., 1996, Ion microprobe analysis of $^{18}O/^{16}O$ in authigenic and detrital quartz in the St. Peter Sandstone, Michigan Basin and Wisconsin Arch, USA: contrasting diagenetic histories: Geochimica et Cosmochimica Acta, v. 60, p. 5101–5116.

Haddad, S.C., Worden, R.H., Prior, D.J., and Smalley, P.C., 2006, Quartz cement in the Fontainebleau Sandstone, Paris Basin, France: crystallography and implications for mechanisms of cement growth: Journal of Sedimentary Research, v. 76, p. 244–256.

Harris, N.B., 1992, Burial diagenesis of Brent sandstones: a study of Statfjord, Hutton and Lyell fields, *in* Morton, A.C., Haszeldine, R.S., Giles, M.R., and Brown, S., eds., Geology of the Brent Group: Geological Society of London, Special Publication 61, p. 351–375.

Haszeldine, R.S., Samson, I.M., and Cornford, C., 1984, Dating diagenesis in a petroleum basin, a new fluid inclusion method: Nature, v. 307, p. 354–357.

Hillier, S., 2003, Quantitative analysis of clay and other minerals in sandstones by X-ray powder diffraction (XRPD), *in* Worden, R.H., and Morad, S., eds., Clay Mineral Cements in Sandstones: International Association of Sedimentologists, Special Publication 34, p. 213–251.

Hogg, A.J.C., Sellier, E., and Jourdan, A.J., 1992, Cathodoluminescence of quartz cements in Brent Group sandstones, Alwyn South, UK North Sea, *in* Morton, A.C., Haszeldine, R.S., Giles, M.R., and Brown, S., eds., Geology of the Brent Group: Geological Society of London, Special Publication 61, p. 421–440.

Hogg, A.J.C., Pearson, M.J., Fallick, A.E., and Hamilton, P.J., 1995, An integrated thermal and isotopic study of the diagenesis of the Brent group, Alwyn South, U.K. North Sea: Applied Geochemistry, v. 10, p. 531–546.

Hower, J., Eslinger, E.V., Hower, M.E., and Perry, E.A., 1976, Mechanism of burial metamorphism of argillaceous sediment: 1. Mineralogical and chemical evidence: Geological Society of America, Bulletin, v. 87, p. 725–737.

Jahren, J., and Ramm, M., 2000, The porosity-preserving effects of microcrystalline quartz coating in arenitic sandstones: Examples from the Norwegian continental shelf, *in* Worden, R.H., and Morad, S., eds., Quartz Cementation in Sandstones: International Association of Sedimentologists, Special Publication 29, p. 271–280.

Kelly, J.L., Fu, B., Kita, N.T., and Valley, J.W., 2007, Optically continuous silcrete quartz cements of the St. Peter Sandstone: High precision oxygen isotope analysis by ion microprobe: Geochimica et Cosmochimica Acta, v. 71, p. 3812–3832.

Kita, N.T., Ushikubo, T., Fu, B., and Valley, J.W., 2009, High precision SIMS oxygen isotope analysis and the effect of sample topography: Chemical Geology, v. 264, p. 43–57.

Kraishan, G.M., Rezaee, M.R., and Worden, R.H., 2000, Significance of trace element composition of quartz cement as a key to reveal the origin of silica in sandstones: an example from the Cretaceous of the Barrow Sub-Basin, Western Australia, *in* Worden, R.H., and Morad, S., eds., Quartz Cementation in Sandstones: International Association of Sedimentologists, Special Publication 29, p. 317–331.

Lander, R.H., and Walderhaug, O., 1999, Predicting porosity through simulating sandstone compaction and quartz cementation: American Association of Petroleum Geologists, Bulletin, v. 83, p. 433–449.

Lander, R.H., Larese, R.E., and Bonnell, L.M., 2008, Toward more accurate quartz cement models: the importance of euhedral versus noneuhedral growth rates: American Association of Petroleum Geologists, Bulletin, v. 92, p. 1537–1563.

Lee, M., and Savin, S.M., 1985, Isolation of diagenetic overgrowths on quartz sand grains for oxygen isotopic analysis: Geochimica et Cosmochimica Acta, v. 49, p. 497–501.

Livera, S.E., 1989, Facies associations and sand-body geometries in the Ness Formation of the Brent Group, Brent Field, *in* Whateley, M.K.G., and Pickering, K.T., eds., Deltas: Sites and Traps for Fossil Fuels: Geological Society of London, Special Publication 41, p. 269–286.

Lynch, F.L., Mack, L.E., and Land, L.S., 1997, Burial diagenesis of illite/smectite in shales and the origins of authigenic quartz and secondary porosity in sandstones: Geochimica et Cosmochimica Acta, v. 61, p. 1995–2006.

Lyon, I.C., Burley, S.D., McKeever, P.J., Saxton, J.M., and Macaulay, C., 2000, Oxygen isotope analysis of authigenic quartz in sandstones: a comparison of ion microprobe and conventional analytical techniques, *in* Worden, R.H., and Morad, S., eds., Quartz Cementation in Sandstones: International Association of Sedimentologists, Special Publication 29, p. 299–316.

Mackenzie, F.T., and Gees, R., 1971, Quartz: synthesis at Earth-surface conditions: Science, v. 173, p. 533–535.

Marchand, A.M.E., Macaulay, C.I., Haszeldine, R.S., and Fallick, A.E., 2002, Pore water evolution in oilfield sandstones: constraints from oxygen isotope microanalyses of quartz cement: Chemical Geology, v. 191, p. 285–304.

McBride, E.F., 1989, Quartz cement in sandstones: a review: Earth-Science Reviews, v. 26, p. 69–112.

Moore, D.M., and Reynolds, R.C.J., 1997, X-Ray Diffraction and the Identification and Analysis of Clay Minerals: New York, Oxford University Press, 378 p.

Morad, S., Ismail, H.N.B., De Ros, L.F., Al-Aasm, I.S., and Serrhini, N.E., 1994, Diagenesis and formation water chemistry of Triassic reservoir sandstones from southern Tunisia: Sedimentology, v. 41, p. 1253–1272.

Oelkers, E.H., Bjørkum, P.A., and Murphy, W.M., 1996, A petrographic and computational investigation of quartz cementation and porosity reduction in North Sea sandstones: American Journal of Science, v. 296, p. 420–452.

Oelkers, E.H., Bjørkum, P.A., Walderhaug, O., Nadeau, P.H., and Murphy, W.M., 2000, Making diagenesis obey thermodynamics and kinetics: the case of quartz cementation in sandstones from offshore mid-Norway: Applied Geochemistry, v. 15, p. 295–309.

Osborne, M., and Haszeldine, S., 1993, Evidence for resetting of fluid inclusion temperatures from quartz cements in oilfields: Marine and Petroleum Geology, v. 10, p. 271–278.

Page, F.Z., Ushikubo, T., Kita, N.T., Riciputi, L.R., and Valley, J.W., 2007, High-precision oxygen isotope analysis of picogram samples reveals 2 μm gradients and slow diffusion in zircon: American Mineralogist, v. 92, p. 1772–1775.

Peltonen, C., Marcussen, Ø., Bjørlykke, K., and Jahren, J., 2009, Clay mineral diagenesis and quartz cementation in mudstones: The effects of smectite to illite reaction on rock properties: Marine and Petroleum Geology, v. 26, p. 887–898.

Pollington, A.D., Kozdon, R., and Valley, J.W., 2011, Evolution of quartz cementation during burial of the Cambrian Mount Simon Sandstone, Illinois Basin: *in situ* microanalysis of $\delta^{18}O$: Geology, v. 39, p. 1119–1122.

Richards, P.C., 1992, An introduction to the Brent Group: a literature review, *in* Morton, A.C., Haszeldine, R.S., Giles, M.R., and Brown, S., eds., Geology of the Brent Group: Geological Society of London, Special Publication 61, p. 15–26.

Thyberg, B., Jahren, J., Winje, T., Bjørlykke, K., Faleide, J.I., and Marcussen, Ø., 2010, Quartz cementation in Late Cretaceous mudstones, northern North Sea: changes in rock properties due to dissolution of smectite and precipitation of micro-quartz crystals: Marine and Petroleum Geology, v. 27, p. 1752–1764.

Vagle, G.B., Hurst, A., and Dypvik, H., 1994, Origin of quartz cements in some sandstones from the Jurassic of the Inner Moray Firth (UK): Sedimentology, v. 41, p. 363–377.

Valley, J.W., and Kita, N.T., 2009, *In situ* oxygen isotope geochemistry by ion microprobe, *in* Fayek, M., ed., Secondary Ion Mass Spectrometry in the Earth Sciences: Gleaning the Big Picture from a Small Spot: Mineralogical Association Canada, Short Course 41, p. 19–63.

Van De Kamp, P.C., 2008, Smectite–Illite–Muscovite transformations, quartz dissolution, and silica release in shales: Clays and Clay Minerals, v. 56, p. 66–81.

Walderhaug, O., 1994, Precipitation rates for quartz cement in sandstones determined by fluid-inclusion microthermometry and temperature-history modeling: Journal of Sedimentary Research 64, p. 324–333.

Walderhaug, O., 1996, Kinetic modeling of quartz cementation and porosity loss in deeply buried sandstone reservoirs: American Association of Petroleum Geologists, Bulletin, v. 80, p. 731–745.

Walderhaug, O., 2000, Modeling quartz cementation and porosity in Middle Jurassic Brent Group sandstones of the Kvitebjørn field, northern North Sea: American Association of Petroleum Geologists, Bulletin, v. 84, p. 1325–1339.

Warren, E.A., and Smalley, P.C., eds., 1994, North Sea Formation Waters Atlas: Geological Society of London, Memoir 15, 208p.

Weibel, R., Friis, H., Kazerouni, A.M., Svendsen, J.B., Stokkendal, J., and Poulsen, M.L.K., 2010, Development of early diagenetic silica and quartz morphologies—examples from the Siri Canyon, Danish North Sea: Sedimentary Geology, v. 228, p. 151–170.

Wilkinson, J.J., Lonergan, L., Fairs, T., and Herrington, R.J., 1998, Fluid inclusion constraints on conditions and timing of hydrocarbon migration and quartz cementation in Brent Group reservoir sandstones, Columba Terrace, northern North Sea, *in* Parnell, J., ed., Dating of Fluid Flow and Fluid–Rock Interaction: Geological Society of London, Special Publication 144, p. 69–89.

Wilkinson, M., Haszeldine, R.S., and Fallick, A.E., 2006, Jurassic and Cretaceous clays of the northern and central North Sea hydrocarbon reservoirs reviewed: Clay Minerals, v. 41, p. 151–186.

Williams, L.B., Hervig, R.L., and Bjørlykke, K., 1997, New evidence for the origin of quartz cements in hydrocarbon reservoirs revealed by oxygen isotope microanalyses: Geochimica et Cosmochimica Acta, v. 61, p. 2529–2538.

Worden, R.H., and Morad, S., 2000, Quartz cementation in oil field sandstones: A review of the key controversies, *in* Worden, R.H., and Morad, S., eds., Quartz Cementation in Sandstones: International Association of Sedimentologists, Special Publication 29, p. 1–2.

Received 12 October 2011; accepted 20 December 2012.